

CONF-8706200--2

RELATIVISTIC HEAVY ION COLLISIONS

M. J. TANNENBAUM

Brookhaven National Laboratory\*  
Upton, N.Y. 11973

BNL--40066

DE87 014292

ABSTRACT

Some of the objectives and observables of Relativistic Heavy Ion Physics are presented. The first experimental results from oxygen interactions at CERN, 200 GeV/c per nucleon, and BNL, 14.5 GeV/c per nucleon are shown. The data indicate more energy emission than was originally predicted.

DISCLAIMER

This report was prepared as an account of work sponsored by an agency of the United States Government. Neither the United States Government nor any agency thereof, nor any of their employees, makes any warranty, express or implied, or assumes any legal liability or responsibility for the accuracy, completeness, or usefulness of any information, apparatus, product, or process disclosed, or represents that its use would not infringe privately owned rights. Reference herein to any specific commercial product, process, or service by trade name, trademark, manufacturer, or otherwise does not necessarily constitute or imply its endorsement, recommendation, or favoring by the United States Government or any agency thereof. The views and opinions of authors expressed herein do not necessarily state or reflect those of the United States Government or any agency thereof.

CEBAF  
1987 Summer Workshop  
June 22-26, 1987  
Invited Talk

\* This research has been supported in part by the U.S.  
Department of Energy under Contract DE-AC02-76CH00016

MASTER

# RELATIVISTIC HEAVY ION COLLISIONS

M. J. TANNENBAUM

Brookhaven National Laboratory\*  
Upton, N.Y. 11973

## ABSTRACT

Some of the objectives and observables of Relativistic Heavy Ion Physics are presented. The first experimental results from oxygen interactions at CERN, 200 GeV/c per nucleon, and BNL, 14.5 GeV/c per nucleon are shown. The data indicate more energy emission than was originally predicted.

## INTRODUCTION

High energy collisions of nuclei provide the means of creating nuclear matter in conditions of extreme temperature and density. At large energy density, or baryon density, a phase transition is expected from a state of nucleons containing confined quarks and gluons to a state of "deconfined" (from their individual nucleons) quarks and gluons covering the entire volume of nuclear matter, or a volume that is many units of the characteristic length scale. This state is expected to be in thermal and chemical equilibrium. In the terminology of high energy physics, this is called a "soft" process, related to the QCD confinement scale

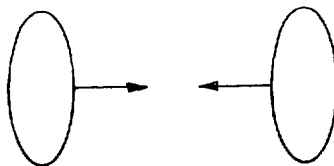
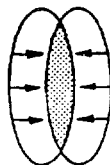
$$\Lambda_{\text{QCD}} \approx 0.1 \text{ GeV} \approx (2 \text{ fm})^{-1}$$

This state is called the Quark-Gluon-Plasma (QGP) [1]

A schematic drawing of a relativistic heavy ion collision is shown in Figure 1. Two energy regimes are discussed for the QGP[2]. At lower energies, typical of the AGS, the colliding nuclei are expected to stop each other, leading to a Baryon-Rich system. This will be the region of maximum baryon density. At very high energy, 100 to 200 GeV per nucleon pair in the center of mass, the nuclear fragments will be well separated from a central region of particle production. This is the region of the Baryon-Free or Gluon plasma.

\* This research has been supported in part by the U.S. Department of Energy under Contract DE-AC02-76CH00016

INITIAL STATE BEFORE COLLISION

 $\sqrt{s}/A \approx 5 \text{ GeV}$ : BARYONS STOPPED IN OVER-ALL CM

AT HIGHER ENERGY, NUCLEI ARE TRANSPARENT TO EACH OTHER

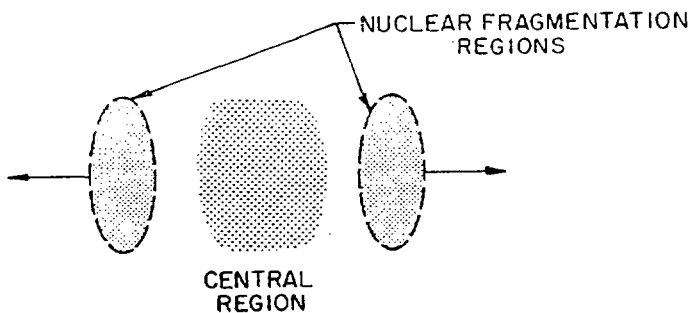


FIGURE 1. Schematic of Relativistic Heavy Ion Collision  
from RHIC Conceptual Design Report BNL 51932(1986)

There has been considerable work over the past few years in making quantitative predictions for the QGP. A recent calculation of a phase diagram for "isentropic expansion trajectories for a hadronizing QGP" [3] is shown below (Figure 2). The transition temperature from a state of hadrons to the QGP varies from  $T_c=140$  MeV at zero baryon density to zero temperature at a critical baryon density  $\sim 6.5$  times the normal nuclear density:

Predictions for the transition temperature are constrained to a relatively narrow range  $140 < T_c < 250$  MeV, while the critical baryon or energy density is predicted to be 5 to 20 times the normal density. [4]

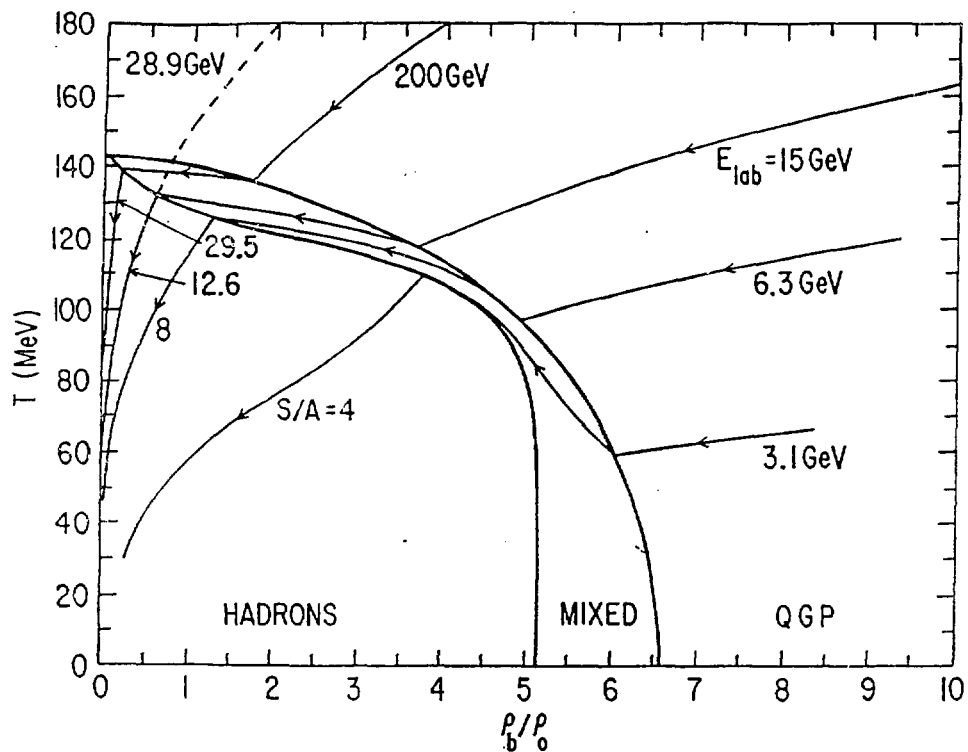


FIGURE 2

From the point of view of an experimentalist there are two major questions in this field. The first is how to relate the thermodynamical properties (temperature, energy density, entropy...) of the QGP or hot nuclear matter to properties that can be measured in the laboratory. The second question is how the QGP can be

detected.

### OBSERVABLES

The challenge of RHI collisions can be understood from Figure 3, which is a streamer chamber photograph of a 200 GeV/u oxygen projectile colliding with a lead nucleus. It would appear to be a daunting task to reconstruct all the particles in such events. Consequently, it is more common to use single-particle or multi-particle inclusive variables to analyze these reactions.

NA 35  $^{16}\text{O} + \text{Pb}$  SEPTEMBER 1986



FIGURE 3

For any particle, the momentum can be resolved into transverse ( $P_t$ ) and longitudinal ( $P_l$ ) components, and in many cases the mass ( $M$ ) of the particle can be determined. The longitudinal momentum distributions are conveniently expressed in terms of the rapidity ( $y$ ):

$$y = \ln[(E+P_l)/M] \rightarrow \eta = -\ln \tan \theta/2 \quad \text{as } M \rightarrow 0$$

$$\cosh y = E/Mt \quad \sinh y = P_l/Mt$$

$$\text{where} \quad Mt = \sqrt{P_t^2 + M^2} \quad \text{and} \quad E = \sqrt{P_l^2 + Mt^2}$$

The transverse momentum distributions can be determined for the different particles, and typically the average transverse momentum,  $\langle Pt \rangle$  is taken as a measure of the temperature,  $T$ . The charged particle multiplicity, either over all space, or in restricted intervals of rapidity, is taken as a measure of entropy.

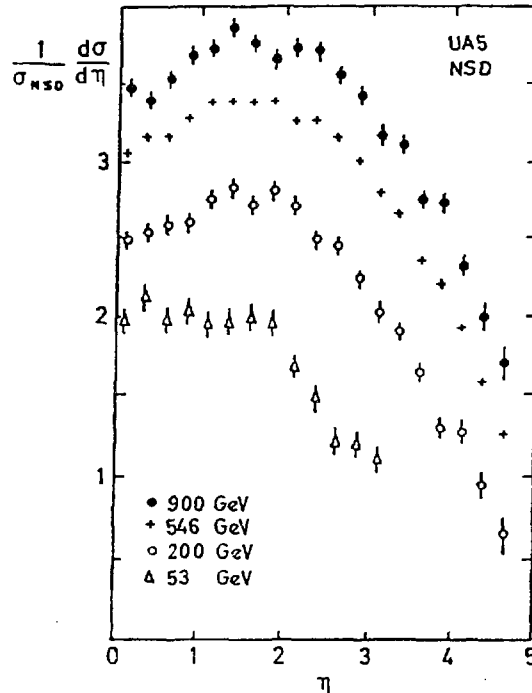


FIGURE 4. Eta is the pseudorapidity ( $M \rightarrow 0$ ) [Ref 1, p148c]

A convenient description of high energy collisions is provided by the charged particle density in rapidity,  $dn/dy$  (Figure 4). Regions of nuclear fragmentation take up the first 1-2 units around the projectile and target rapidity and if the center-of-mass energy is sufficiently high, a central plateau is exhibited. Another, similar variable is the transverse energy density in rapidity or  $dEt/dy = \langle pt \rangle * dn/dy$ . This is thought to be related to the co-moving energy density in a longitudinal expansion, and according to Bjorken [5] is proportional to the energy density in space  $\epsilon$ :

$$\epsilon = \frac{dEt/dy}{\pi R^2 \tau}$$

where  $\tau$  is the formation time - 1 fm.

## SIGNATURES OF THE QUARK-GLUON-PASMA

One of the more interesting signatures proposed for the QGP is that it could trigger a catastrophic transition from the metastable vacuum of the present universe to a lower energy state, " a possibility naturally occurring in many spontaneously broken quantum field theories " [6]. A more likely outcome is that the existence of the QGP will be inferred from a comprehensive and systematic set of experimental data exhibiting several striking features or "anomalies", "which can be interpreted in a unified way as manifestations of QGP production" [7]. Examples of the features expected for the QGP and signatures to find them are given below:

## a) CHARACTERISTIC TEMPERATURE ENTROPY CURVE: [8]

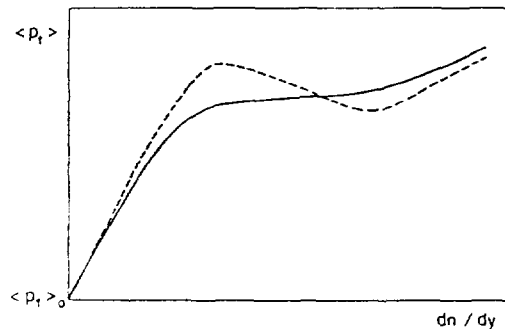


FIGURE 5

Note that this curve has the features of a phase transition with which we are all familiar. The  $\langle P_t \rangle$ , acting as temperature, increases with increasing entropy ( $dn/dy$ ); then as the phase transition takes place (e.g. water changing to steam) the temperature remains constant and begins rising again when the transition to the new phase is complete.

## b) PLASMA DROPLETS CAUSED BY DEFLAGRATION: [9]

These would be manifested by large fluctuations in  $dn/dy$  or  $dE_t/dy$  covering a range of  $\sim 1$  unit on an event by event basis. The hope would be to observe the other plasma signatures only in the region of the fluctuation and not in the other regions.

## c) THERMAL EQUILIBRIUM:

One of the best probes of thermal equilibrium is lepton pair production [10]. There are two characteristic

features of thermal production of lepton pairs. The number of lepton pairs per unit of rapidity is proportional to the square of charged particle density, and furthermore this ratio is proportional to the transition temperature  $T_c$ :

$$\frac{dN_{\mu^+\mu^-}/dy}{(du/dy)^2 \times 10^{-7}} = 15 T_c \text{ (GeV)}$$

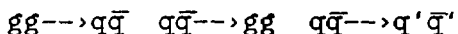
Also, the Pt and mass dependence of the cross section are not independent but depend only on the transverse mass Mt. This means that at any fixed value of M, the  $\langle Pt(M) \rangle$  is linearly proportional to M.

d) VOLUME OF THERMAL MATTER:

The size of the thermal source is thought to be measured by identical particle interferometry using the GGLP effect [11]. When two identical pions occupy nearly the same coordinates in phase space, the amplitudes interfere constructively due to the symmetry of the wave-function imposed by Bose-Einstein statistics. The characteristic momentum difference leading to decorrelation in momentum space can be measured, and is taken to be the fourier transform of the size of an extended source in position space. It should be noted that dynamical effects due to final state interactions can be large, and make the interpretation of such measurements a very specialized subject [12].

e) CHEMICAL EQUILIBRIUM [13,14]:

In the QGP there will be gluons, quarks and anti-quarks. They will continuously react with each other via the QCD subprocesses:



where  $q'$  represents a different flavor quark (u, d or s). After several interactions have taken place, the reaction rates and the abundances of the gluons and the different flavor quarks (and anti-quarks) will become equilibrated, so that they no longer change with time. This is called chemical equilibrium. Since the transition temperature  $T_c$  is comparable to the strange quark mass -150 MeV, the strange quarks  $s, \bar{s}$  should have the same abundance as the  $u, \bar{u}$  and  $d, \bar{d}$  in the gluon plasma. In the baryon-rich plasma, the  $s, \bar{s}$  will be enhanced compared to u and d since  $u, \bar{u}$  and  $d, \bar{d}$  are "Pauli" blocked by valence u and d quarks.

The principal probe of chemical equilibrium is the

particle composition. For instance, the abundance of strange mesons and baryons as well as anti-baryons should be quite different in a QGP than in a hadron gas or in an ordinary nuclear collision

f) DECONFINEMENT :

It has recently been proposed [15] that  $J/\Psi$  production in A+A collisions will be suppressed by Debye screening of the quark color charge in the QGP. The  $J/\Psi$  is produced when two gluons interact to produce a  $c, \bar{c}$  pair which then resonates to form the  $J/\Psi$ . In the plasma the  $c, \bar{c}$  interaction is screened so that the  $c, \bar{c}$  go their separate ways and eventually pick up other quarks at the periphery to become "open charm". This would be quite a spectacular effect since the naive expectation is that  $J/\Psi$  production, being a pointlike process, should go like  $A^2$  in an A+A collision, and thus would be enhanced relative to the total interaction cross section, which increases only as  $A^{2/3}$ .

### EXPERIMENTAL TECHNIQUES

Each of the probes of the QGP tends to have a different experimental technique associated with it. In all cases the multiplicities in nuclear collisions are so large that all the detectors used are very highly segmented. For measuring the charged multiplicity or  $dn/dy$  a segmented multiplicity detector is used, usually an array of proportional tubes with pad readout, or a silicon pad array. For measuring transverse energy flow,  $dE_t/dy$ , a hadron calorimeter is used. Some groups use an electromagnetic shower counter for this purpose. This has the advantage of being smaller, cheaper and higher in resolution than a full hadron calorimeter; but has the disadvantage of being biased, since only  $\pi^0$  and  $\eta$ - $\pi^0$  mesons are detected (via their two photon decay). Nuclear fragmentation products are detected by calorimeters in the projectile direction and by E,  $dE/dx$  scintillator arrays in the target fragmentation region. The particle composition and transverse momentum distributions are measured using magnetic spectrometers with particle identification. Typically, time-of-flight, gas and aerogel Cerenkov counters, and  $dE/dx$  are used to separate pions from kaons, protons, deuterons, etc. Drift chambers are generally utilized for charged particle tracking, although streamer chambers and time projection chambers (TPC) are also in use. Lepton pair detectors are very specialized, and usually combine

magnetic spectrometers with lepton identification (muons by penetration, and electrons by "gas" and "glass").

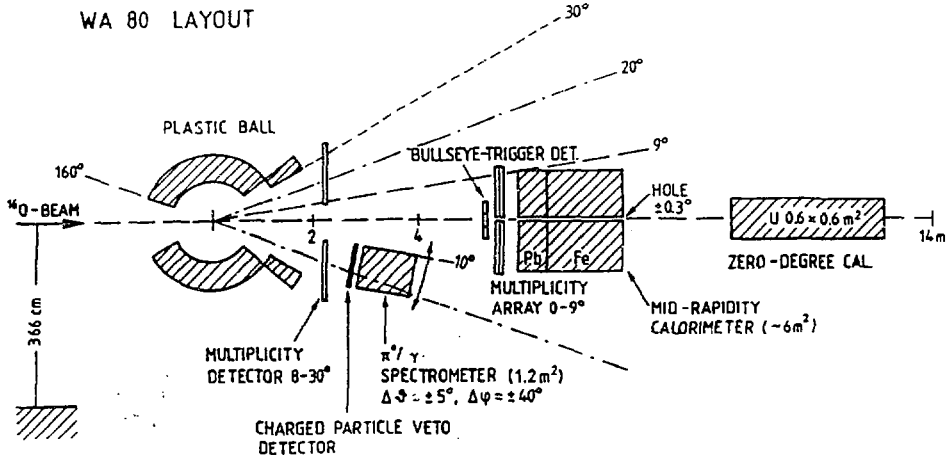
One of the specific problems in this field is how to detect, with minimum bias, when a nucleus-nucleus collision has taken place. Two techniques are used. The first is to put a calorimeter at zero degrees to determine whether the projectile has the full beam energy or has lost some energy. The second uses a so-called bullseye counter downstream of the target, sized just large enough to detect all the beam particles. The bullseye also measures the charge of the beam particles since the pulse height is proportional to  $Z^2$ . If a particle misses the bullseye, or the charge changes, this is taken as an indication of a nuclear interaction.

With that quick overview of the experimental techniques, the following "photo album" of the first round of experiments at CERN and Brookhaven should be easier to comprehend. The CERN heavy ion program provides oxygen beams at 60 and 200 GeV/u and will eventually improve the source to provide sulfur and possibly lead beams. There are 5 major experiments: WA80 (Figure 6), NA34 (Figure 7), NA35 (Figure 8), NA36 (Figure 9), and NA38 (Figure 10). The BNL heavy ion program has provided oxygen and silicon beams at 14.5 GeV/c per nucleon and is scheduled to accelerate gold beams in 1989. A major improvement is planned for 1995 when RHIC is scheduled to begin operation. RHIC will provide colliding beams, covering the full mass number spectrum, with center-of-mass energies from 5 to 200 GeV per nucleon pair. At present, there are 3 major RHI experiments at the BNL-Tandem-AGS: E802 (Figure 11), E810 (Figure 12) and E814 (Figure 13).

#### FIRST EXPERIMENTAL RESULTS

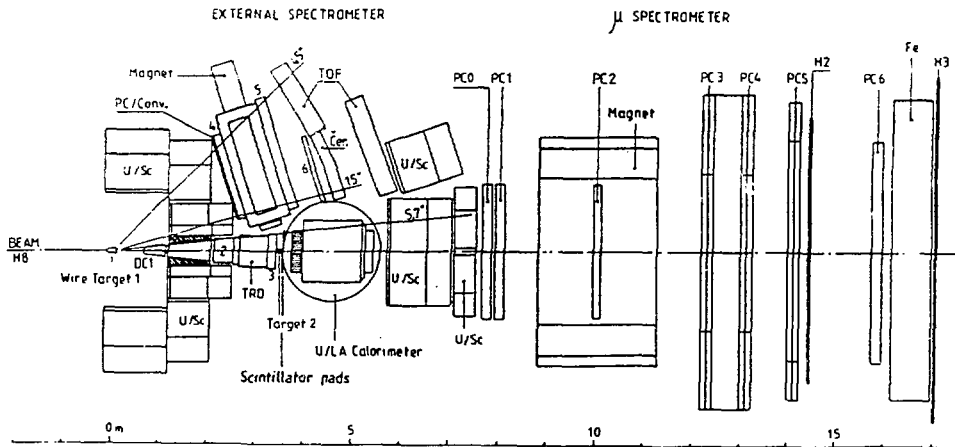
CERN had a very successful oxygen run in the fall of 1986, and already one experimental result has been published [16]. At BNL, some time was made available for physics during machine studies with oxygen in the fall of 1986 and routine running began in the spring of 1987 with a silicon beam. No results are available yet from the silicon run, but a small test experiment using the oxygen beam will be reported [17]. Results on heavy ion collisions from cosmic rays [18] and from the Bevalac [19] have also been published this year but are beyond the scope of this article.

CERN PROGRAM



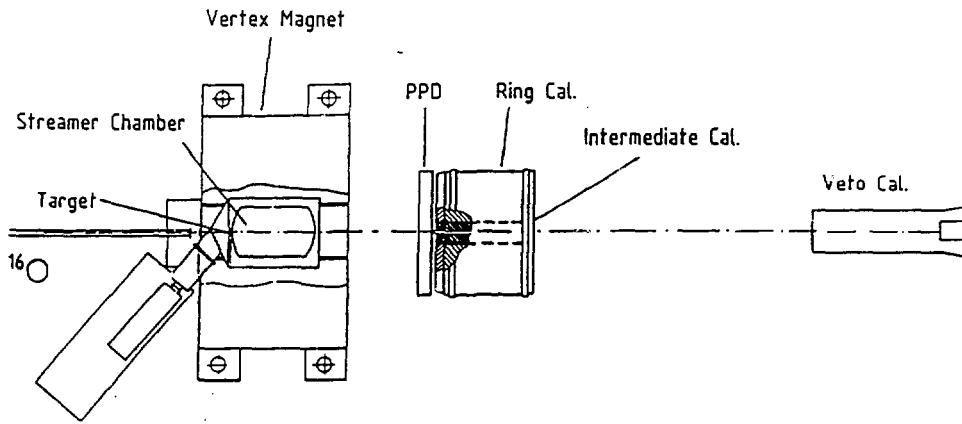
Experiment WA80: Study of Relativistic Nucleus-Nucleus Collisions at the CERN SPS

FIGURE 6



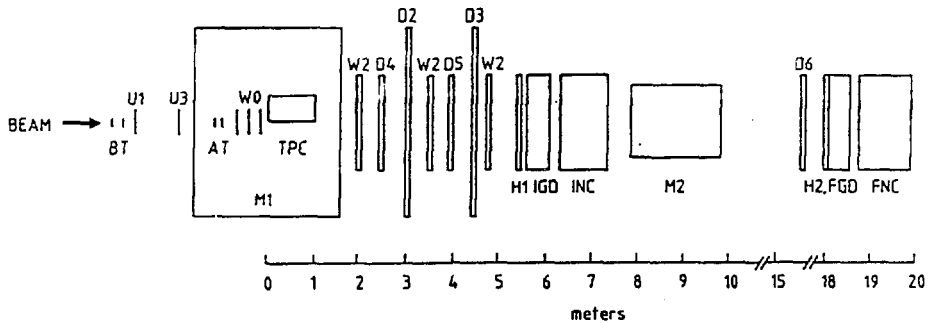
Experiment NA34/2: Study of High Energy Densities over Extended Nuclear Volumes via Nucleus-Nucleus Collisions at the SPS

FIGURE 7



Experiment NA35: Study of Relativistic Nucleus-nucleus Collisions

FIGURE 8



BT = beam tag  
 AT = active target  
 M1 M2 = magnets  
 H1 H2 = hodoscopes  
 IGD, FGD = gamma detectors  
 INC, FNC = hadron calorimeters

U1, U3 } prop. wire chamber  
 W0, W2 }  
 D2 - D6 = drift chambers

Experiment NA36: Production of Strange Baryons and Antibaryons in Relativistic Ion Collisions

FIGURE 9

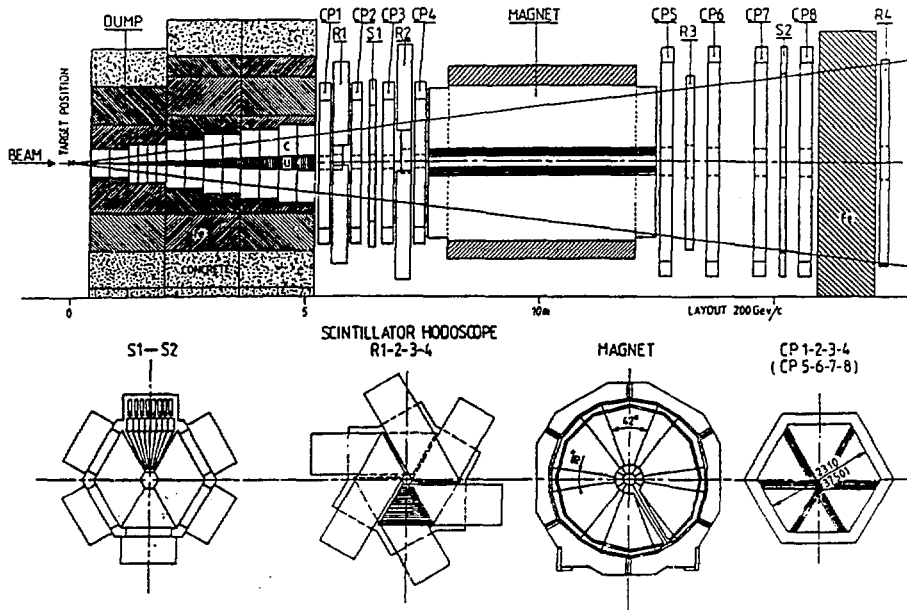


FIGURE 10. NA38 Study of High-Energy Nucleus-Nucleus Interactions with the Enlarged NA10 Dimuon Spectrometer

BNL-TANDEM-AGS PROGRAM

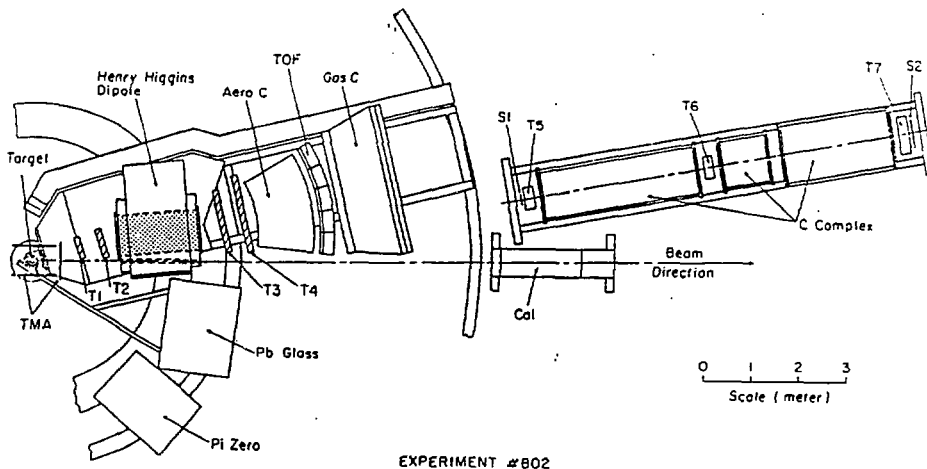


FIGURE 11. E802 Studies of Particle Production at Extreme Baryon Densities in Nuclear Collisions at the AGS

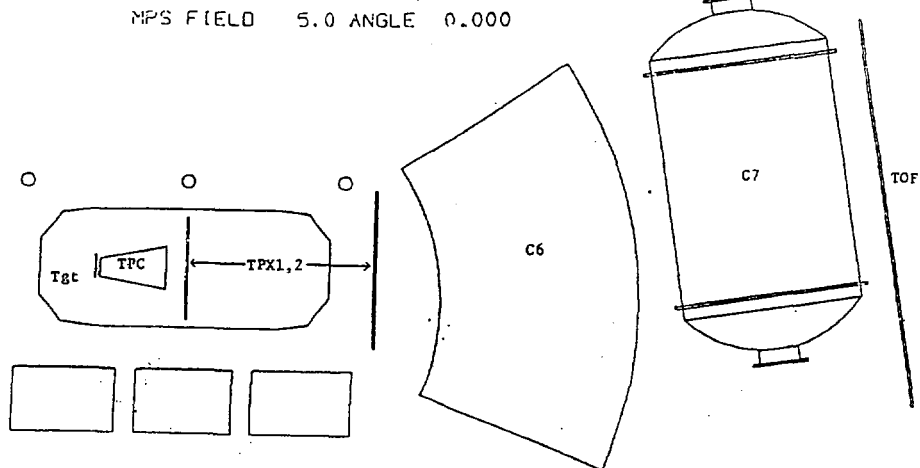


FIGURE 12. E810 A Search for Quark Matter (QGP) and other New Phenomena Utilizing Heavy Ion Collisions at the AGS

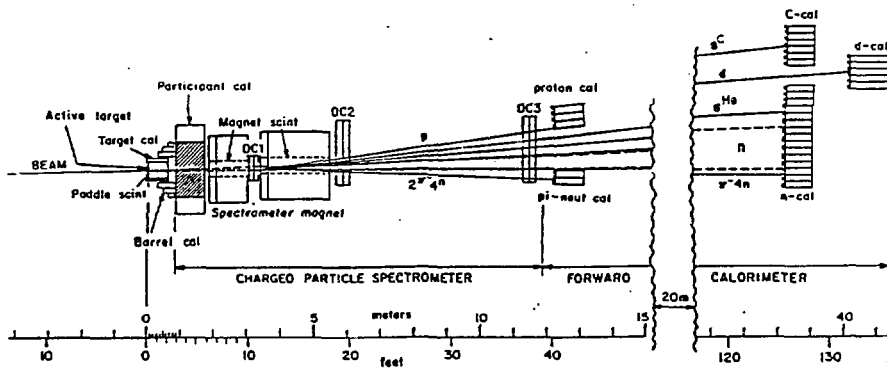


FIGURE 13. E814 Study of Exotic Nuclear States Via Coulomb or Diffractive Projectile Excitation

The NA35 experiment (Figure 8) uses a streamer chamber to detect all the charged particles emerging from an interaction as well as the neutral strange particles that decay inside the chamber. A ring-shaped hadron calorimeter and a shower counter (PPD) are used to measure the transverse energy in the lab rapidity interval  $2.2 < y(\text{lab}) < 3.8$ , corresponding to approximately  $-0.8 < y < 0.8$  in the nucleon-nucleon c.m. system. The energy degradation of the oxygen projectile is measured using a zero degree veto calorimeter, which is also used for triggering. A streamer chamber photograph from this experiment was already shown above (Figure 3). Measurements of the mean charged particle multiplicity (for angles forward of 60 degrees) are shown in figure 14 as a function of the energy observed in the veto calorimeter. As the energy observed in the veto calorimeter decreases, the mean charged particle multiplicity increases, reaching a value of 260.

Very striking results have been obtained from the differential spectrum in transverse energy observed in the ring-calorimeter and PPD. In figure 15 the Et spectrum from the interactions of 200 GeV/u oxygen in a lead target is shown together with the Et spectrum from 200 GeV proton interactions in an Au target measured with the same setup. A most interesting feature of this data is that the 16-fold convolution of the measured p+Au spectrum beautifully reproduces the high energy edge of the O+Pb spectrum. This observation has been confirmed by the E802 collaboration at Brookhaven.

As one of the first major experiments scheduled at the Tandem-AGS, E-802 took data with a silicon beam in spring 1987 in the configuration shown in Figure 11. In addition, during the machine development run in the fall of 1986, a small test experiment was assembled from components of E802, and measurements were made using an oxygen beam of momentum 14.5 GeV/c per nucleon. The setup of the test experiment is shown in a photograph (figure 16). An array of 96 lead glass blocks (PbGl) was placed 1 meter downstream of the target. The array was 10 blocks wide by 10 high with a 2 by 2 block hole in the center for the beam to pass through. The PbGl array measured the electromagnetic energy emitted in a laboratory polar angular interval from 10 to 32 degrees, with full azimuthal coverage. In the nucleon-nucleon center of mass reference frame, this corresponds to a rapidity coverage of  $-0.5 < y < 0.7$  for massless particles. Triggers were provided by a bullseye counter or by an

FIGURE 14

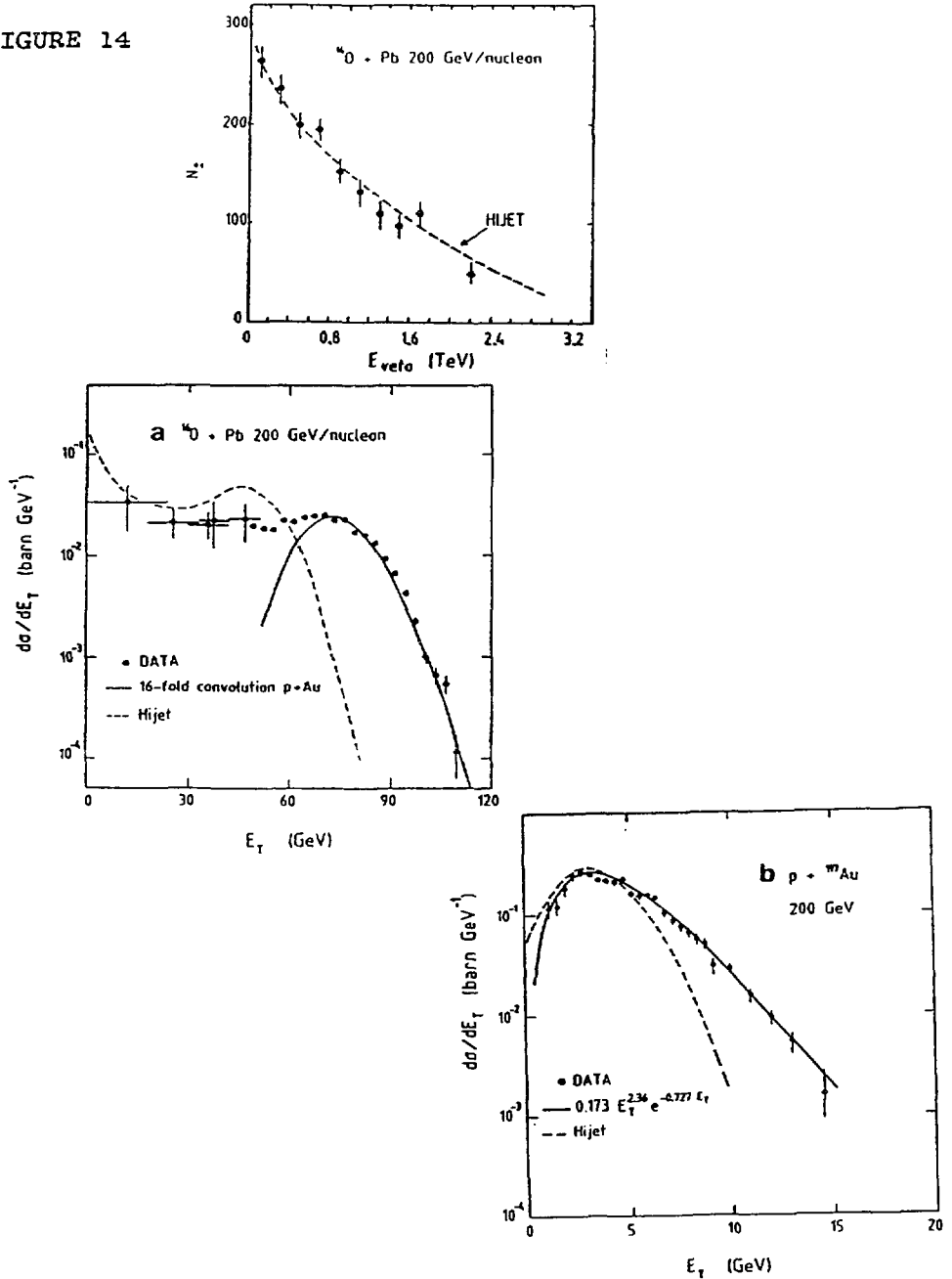


FIGURE 15. NA35 Et spectra for O+Pb and p+Au at 200 GeV/u

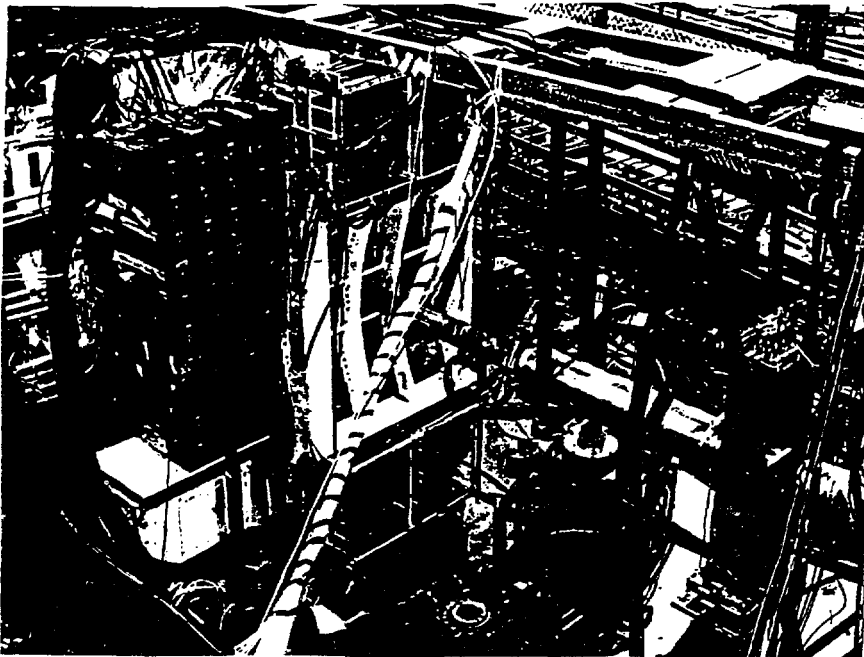


FIGURE 16. E802 test setup for oxygen runs.

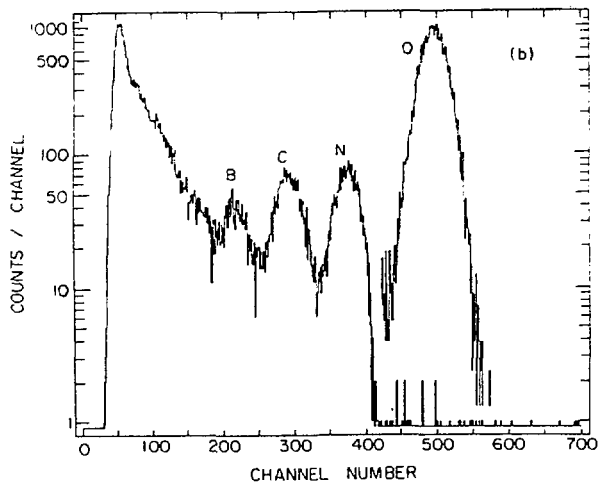


FIGURE 17. E802 Spectrum in Bullseye counter.

analog sum of the outputs of the 96 PbGl photomultipliers, corresponding to the total energy recorded with no transverse weighting. The pulse height spectrum observed in the bullseye counter is shown in figure 17. The oxygen peak is obtained from a sample of non-interacting beam particles, and superimposed onto the data from the PbGl triggers. When energy is observed in the PbGl, the oxygen peak vanishes and is replaced by peaks corresponding to nitrogen, carbon and boron as well as a dominant continuum.

The spectrum of energy observed in the PbGl is shown in figure 18 for oxygen interactions in on Au, Cu, and mylar targets and proton interactions on an Au target, all measured at 14.5 GeV/c per nucleon in the same setup. The observed energy is denoted  $E_{tot}$  since it is primarily the result of production of multiple neutral mesons,  $\pi^0$  and  $\eta^0$ , which are detected via their two-photon decay. Relativistic charged hadrons also emit Cerenkov light in the PbGl, approximately 500 MeV per particle, and contribute, on the average, about 50% of the observed energy. The  $E_{tot}$  spectrum for O+Au shows a peak centered at 40 GeV and then a sharp drop-off until the yield runs out at  $\sim 70$  GeV. The O+Cu data also show evidence of considerable energy emission, even though the maximum thickness of a Cu nucleus is only  $\sim 2/3$  that of Au. It is of particular interest that the edges of the O+Au and O+Cu spectra become virtually identical above 50 GeV if the Cu cross section is multiplied by a factor of  $\sim 6$ .

These features can be described by a simple, geometrical model, based on the observation made at CERN (Figure 15) that the high energy edge of the O+Au (Pb in their case) is just the 16-fold convolution of the p+Au spectrum. This model can be extended to describe the entire O+Cu and O+Au spectra. The observed p+Au spectrum is convoluted from 1 to 16 times, with weights for the  $n$ -fold convolutions obtained from a geometrical calculation which averages over the impact parameter of the nucleus-nucleus collision to obtain the distribution in the number of projectile nucleons which interact at least once in the target. Woods-Saxon densities are assumed for both the projectile and target nuclei and a p-p inelastic cross section of 30 mb is used, corresponding to a nucleon-nucleon mean free path of  $\sim 2.2$  fm.

Surprisingly good representations of both the O+Cu

FIGURE 18  
E802 Data

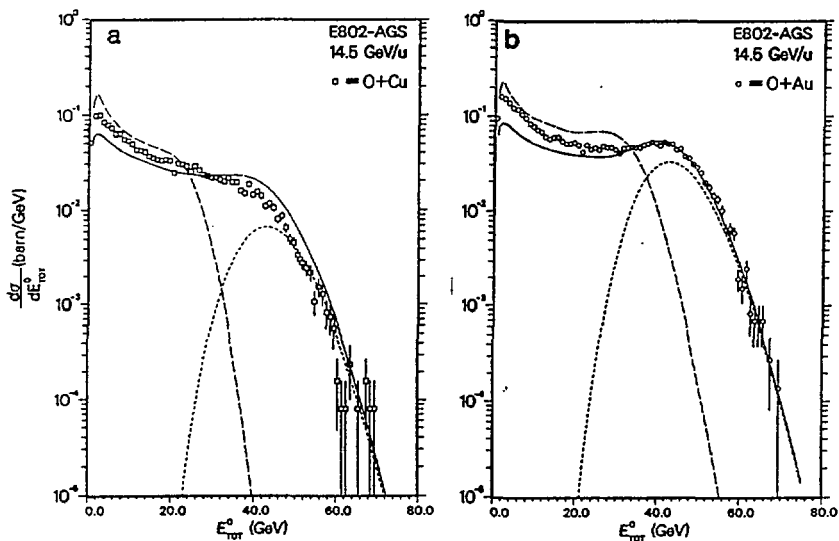
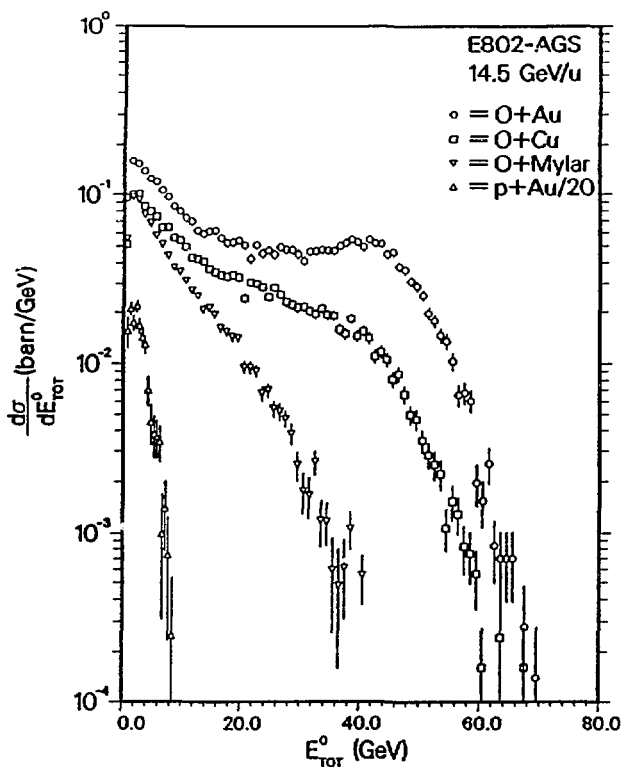


FIGURE 19. E802 Data with Fits as described in text.

and O+Au spectra are obtained from this "wounded-projectile-nucleon" model (Figure 19, solid lines). It then becomes clear that the peak in the O+Au spectrum and the identical shape of the high-energy edges of the O+Au and O+Cu spectra arise from events in which all 16 projectile nucleons interact in the target (Figure 19, dotted lines).

While seemingly reasonable, this naive model is in severe contradiction with the understanding of relativistic nuclear interactions gleaned from proton-nucleus collisions. When a proton passes through a nucleus, it can make several successive interactions. However, the observed  $dn/dy$  in p+A collisions is not simply proportional to the number of collisions but increases much more slowly. For instance, in a p+Au collision there are on the average 4.2 nucleon-nucleon interactions but the observed multiplicity density increases only by a factor of 2. Most of the effort in theories of the collisions of protons with nuclei has gone into trying to understand how the effects of the successive interactions are suppressed [20,21].

In general, the models for this suppression contain the same common features. When a relativistic nucleon interacts, it becomes an excited nucleon, and remains in that state inside the nucleus because time dilation prevents it from fragmenting into particles until it is well outside the nucleus. This feature immediately eliminates the possibility of a cascade in the nucleus from reinteraction of the secondary fragments. Furthermore it is usually assumed 1) that the excited nucleon interacts with the same cross section as an unexcited nucleon and 2) that the "fragmentation stage is independent of the number of interactions involved in the first stage" [20,22].

These features are epitomized in the wounded nucleon model (WNM) [23,24]. In this model the number of nucleons struck in a collision is computed geometrically (as above); but a nucleon contributes only once to the production of particle no matter how many times ( $>1$ ) it is successively struck. Another model called HIJET [25] is frequently discussed. HIJET suppresses the effect of successive collisions by allowing only the leading baryon from an excited nucleon to interact sequentially. The suppression occurs because the leading baryon loses  $\sim 1/2$  of its energy per interaction, so that the available energy is reduced on each successive interaction. Both

these models work well for p+A collisions, but fail to describe the first results for 160 collisions in nuclei (Figure 15, broken line, HIJET), (Figure 19, broken line, WNM). The failure is particularly striking for the O+Cu data from E802.

It is not difficult to understand the reason for the failure of these models in nucleus-nucleus collisions. The effect of projectile nucleons making successive collisions in the target has been suppressed, based on the proton-nucleus data. By the same token, the effect of target nucleons making successive collisions with projectile nucleons is also suppressed in these models, leading to a prediction of much lower energy emission in O+Au collisions than is actually observed. The naive model discussed above overcomes this problem by allowing a seeming contradiction: the effect of successive interactions of projectile nucleons in the target is suppressed (by utilization of the observed p+Au spectrum), whereas the case when target nucleons are successively struck by multiple nucleons from the projectile is not suppressed, but the effect is taken as linear in the number of interactions, as apparently indicated by the measurements.

This is all very exciting. The seeming contradictions will have to be sorted out by the theorists. Meanwhile, the experimentalists will take more data and find new contradictions. The opportunities for discovery are large, as befits a new field of research. To get a feeling for the state of the field, I quote the conclusion given by Tatsuo Matsui in a recent seminar at BNL: "The study of ultrarelativistic heavy ion collisions is a tremendously exciting and rich subject. It addresses a deep and fundamental question in the physical world; and requires an integrated use of expertise from many disciplines in Physics. It is a challenging and thrilling new frontier of Nuclear Physics. We need RHIC"

## REFERENCES

- [1] Proceedings of the Fifth International Conference on Ultra-Relativistic Nucleus-Nucleus Collisions, Quark Matter '86, Nucl. Phys. A461,1c-538c (1987); and previous proceedings in this series.
- [2] R.Anishetty, P.Koehler & L.McLerran, Phys. Rev. D22,2793(1980)
- [3] U.Heinz et al, Phys. Rev. Lett. 58,2292(1987)
- [4] G.Baym & S.A.Chin, Phys. Lett. 62B,241(1976); G. Chapline & M.Nauenberg, Phys. Rev. D16,450(1977); H.Satz, Ann. Rev. Nucl. Part. Sci. 35,245(1985)
- [5] J.D.Bjorken, Phys. Rev. D27,140(1983)
- [6] P.Hut, Nucl. Phys. A418,301c(1984)
- [7] L.Van Hove, Ref. 1, pp 3c-10c.
- [8] L.Van Hove, Phys. Lett. 118B,138(1982)
- [9] L.Van Hove, Z.Phys. C21,93(1983)
- [10] R.Ewa & K.Kajantie, Phys. Rev. D32,1109(1985); K.Kajantie, J.Kapusta, L.McLerran & A.Mekjian Phys. Rev. D34,2746(1986)
- [11] G.Goldhaber, S.Goldhaber, W.Lee & A.Pais, Phys. Rev. 120,300(1960)
- [12] M.Gyulassy, Phys. Rev. Lett. 48,454(1982)
- [13] J.Rafelski & B.Muller, Phys. Rev. Lett. 48,1066(1982)
- [14] T.Matsui, B.Svetitsky & L.McLerran, Phys. Rev. D34,2047(1986)
- [15] T.Matsui & H.Satz, Phys. Lett. B178,416(1986)
- [16] NA35 Collab., A.Bamberger et al, Phys. Lett. B184,271(1987)
- [17] E802 Collab., T.Abbott et al, submitted to Phys. Lett.
- [18] T.H.Burnett et al, Phys. Rev. Lett. 57,3249(1986)
- [19] J.W.Harris et al, Phys. Rev. Lett. 58,463(1987)
- [20] P.M.Fishbane & J.S.Trefil, Phys. Rev. D9,168(1974); Phys. Lett. 51B,139(1974); K.Gottfried, Phys. Rev. Lett. 32,957(1974)
- [21] W.Busza et al, Phys. Rev. Lett. 34,836(1975)
- [22] S.Date, M.Gyulassy & H.Sumiyoshi, Phys. Rev. D32,619(1985)
- [23] A.Bialas, A.Bleszynski & W.Czyz, Nucl. Phys. B111,461(1976)
- [24] H.Brody, S.Frankel, W.Frati & I.Otterlund, Phys. Rev. D28,2334(1983)
- [25] T.W.Ludlam, BNL Report 51921,373(1985)